ARTICLE NO. 77-387R

# Impact Induced Stress Waves in an Anisotropic Plate

Byoung Sung Kim* and Francis Moon†
*Cornell University, Ithaca, N.Y.*

**Stress wave propagation in an anisotropic plate due to impact forces has been examined. The plate is modeled as a number of identical anisotropic layers. Mindlin's approximate theory of plates is applied to each layer to obtain a set of difference-differential equations of motion with use of the interlaminar stresses and displacements as explicit variables. Dispersion relationships for harmonic waves are found when traction-free boundary conditions are applied to both surfaces of the plate and appropriate correction factors are found. The difference-differential equations are reduced to difference equations via integral transforms. With given impact boundary conditions, these equations are solved for an arbitrary number of layers in the plate and the transient propagation of stress waves is calculated by means of a Fast Fourier Transform algorithm.**

## Nomenclature

| | |
|---|---|
| $a, t_0$ | = impact width and time |
| $b=\Delta/2N$ | = a half of layer thickness |
| $c_{ijkl}, c_{ij}\,(C_{ij})$ | = elastic moduli (normalized by $c_{66}$) |
| $f=b\Delta\rho/c_{66}T_0^2$ | = normalization factor |
| $k$ | = wave number (variable of Fourier transform on $\eta$) |
| $N$ | = number of layers in the plate |
| $s$ | = variable of Laplace transform on $\tau$ |
| $T_0=a/(c_{66}/\rho)^{1/2}$ | = normalization time unit |
| $u_i$ | = displacement vector |
| $u_n\,(U_n), v_n\,(V_n)$ | = displacement components at layer interfaces (normalized by $\Delta$) |
| $x_i, t$ | = space and time variables |
| $\Delta$ | = plate thickness |
| $\epsilon_{ij}, \epsilon_i$ | = infinitesimal strain tensor |
| $\rho$ | = density |
| $\sigma_{ij}, \sigma_i$ | = stress tensor |
| $\sigma_n\,(\Sigma_n), \tau_n\,(T_n)$ | = stress at layer interfaces (normalized by $c_{66}$) |
| $\eta=x_1/\Delta, \xi=x_2/b,$ $\tau=t/T_0$ | = normalized space and time variables |

## I. Introduction

RECENTLY, problems of stress wave propagation in a composite plate have attracted much interest because of its important applications in aerospace industries. The present research is a continuation of our previous effort in this field.[1-4]

Because of the inhomogeneity of materials and the complexity of structure geometry, exact theoretical predictions of deformation states of composite plates are seldom possible. The simplest approach is to replace the composite by a homogeneous material of an effective modulus with a minimal consideration of the internal structure, as suggested by White and Angona.[5] An alternative model, proposed by Sun et al.,[6] consists of two alternating homogeneous layers of different elastic properties known as the effective stiffness model. For a certain class of problems, the effective modulus theory works reasonably well. But for a high-frequency dynamic problem, the effective stiffness theory is known to be more accurate, particularly when the wavelength is comparable with some internal characteristic length, such as fiber diameter or layer thickness.

The next level of approximation is plate theory; namely, the displacement field is approximated by a few leading terms of a series expansion in terms of the thickness variables. A power series expansion by Mindlin,[7] a Legendre polynomial expansion by Mindlin and Medick,[8] and a trigonometric expansion by Lee and Nikodem[9] have been successfully applied. Depending on the problem, it is sometimes useful to invent mode functions by a combination of a few basic modes,[10] as in a finite-element method.

Extension of the preceding works to transient wave problems can usually be achieved by finding a number of dispersion relations with the corresponding eigenfunction and by calculation of the transient solution as a linear combination of the eigensolutions.[11,12] But in many cases, finding dispersion relations and modal solutions is in itself difficult. The accuracy of such approximate solutions obviously depends on the number and accuracy of the modal solutions.

In this paper we present a new attempt to examine transient wave propagation in a plate due to impact by employing a multilayer model for a homogeneous anisotropic plate. The plate is imagined to consist of $N$ identical anisotropic layers. A set of governing differential equations of motion is obtained for each layer by application of the approximate plate theory of Mindlin[8] to the layer. Displacement and stress components on the layer surface are explicit unknown variables. Application of continuity conditions of stress and displacement at layer interfaces yields difference-differential equations of motion as a result of the simple periodic structure of the plate. These become a set of simultaneous difference equations after a double integral transform. This technique for analysis of a periodic structure has been widely used in the study of electric transmission lines[13] and in vibrations of multistory buildings.[14] After the complete solutions have been computed in a frequency-wave number space, the stress and displacement fields can be calculated by inversions of integral transforms using the Fast Fourier Transform (FFT) algorithm.

The advantages of this method lie in the use of a difference equation formulation and application of the FFT. Because of the periodic structure, the difference equations always remain the same regardless of the number of layers in the plate; neither algebraic complexity nor numerical disadvantage is incurred when the number of layers is increased. Fur-

Presented as Paper 77-387 at the AIAA/ASME 18th Structures, Structural Dynamics and Materials Conference, San Diego, Calif., March 21-23, 1977; submitted Aug. 8, 1977; revision received March 28, 1979. 

Index categories: Structural Dynamics; Structural Composite Materials.

*Research Associate, Dept. of Theoretical and Applied Mechanics; presently, Member of Research Staff, Engineering Research Center, Western Electric Co., Princeton, N.J. Member AIAA.

†Associate Professor, Dept. of Theoretical and Applied Mechanics.

thermore, the application of the FFT enables one to efficiently sum solutions either in a frequency or wave number space in order to obtain the transient solution.

Results are presented in this paper for a line impact on an infinite anisotropic plate with effective elastic properties of a graphic-epoxy composite. The technique can be extended to a full three-dimensional impact problem.

## II. Formulation

### Basic Theory of Linear Anisotropic Elasticity

Cauchy's equations of motion in Cartesian tensor form without body forces are given by

$$\sigma_{ij,i}=\rho\ddot{u}_j \tag{1}$$

where the repeated index implies summation on that index. A comma represents partial differentiation with respect to the index following the comma and a superposed dot represents a time derivative. The infinitesimal strain tensor $\epsilon_{kl}=\frac{1}{2}(u_{k,l}+u_{l,k})$ is related to the stress tensor by

$$\sigma_{ij}=c_{ijkl}\epsilon_{kl} \quad \text{or} \quad \sigma_i=c_{ij}\epsilon_j \tag{2}$$

For two-dimensional orthotropic materials, $c_{ij}$ is given by

$$c_{ij}=\begin{bmatrix} c_{11} & c_{12} & 0 \\ c_{12} & c_{22} & 0 \\ 0 & 0 & c_{66} \end{bmatrix} \tag{3}$$

### Analysis of a Layer

For an arbitrary layer shown in Fig. 1, we employ the approximate plate theory of Mindlin.[4,8] The displacement field $u$ is expanded in the layer thickness in terms of Legendre polynomials,

$$u(x_1,x_2,x_3,t)=\sum_{n=0}^{\infty} u^{(n)}(x_1,x_3,t)P_n(\xi) \tag{4}$$

where $\xi$ is the local coordinate in the thickness direction normalized by $b$, a half of the layer thickness.

Instead of solving Eq. (1) directly, we solve new approximate equations of motion which are obtained through a variational process by integration of Eq. (1) over the thickness. The result is[1,8]:

$$b\sigma^{(n)}_{\alpha j,\alpha}+[P_n(\xi)\cdot\sigma_{2j}]^{1}_{\xi=-1}-\sigma^{*(n)}_{2j}=\frac{2\rho b}{2n+1}\ddot{u}^{(n)}_j \tag{5}$$

where

$$\sigma^{(n)}_{\alpha j}=\int_{-1}^{1} P_n(\xi)\cdot\sigma_{\alpha j}\,d\xi \qquad \alpha=1,3$$

$$\sigma^{*(n)}_{2j}=\int_{-1}^{1}\frac{dP_n(\xi)}{d\xi}\sigma_{2j}\,d\xi \qquad j=1,2,3 \tag{6}$$

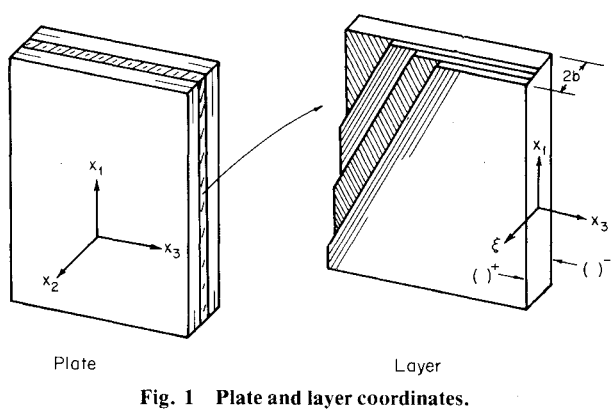


Fig. 1 Plate and layer coordinates.

By substituting the constitutive relation (2), with the displacement expansion (4) into the preceding approximate equations of motion, we can find governing equations of motion in terms of $u^{(0)}_1$, $u^{(0)}_2$, $u^{(0)}_3$, $u^{(1)}_1$.... The accuracy of this approximate theory depends on how many terms of the displacement field we retain. Since the complexity in formulation increases rapidly with the number of terms included, we keep terms only up to second order. We will examine waves propagating in the $x_1$ and $x_2$ directions due to an infinitely long line impact on the $x_3$ axis at $x_2=-b$. Therefore, $u_3=u_{i,3}=\sigma_{ij,3}=0$. To eliminate undesired coupling with higher modes, we set $\ddot{u}^{(2)}_1=\ddot{u}^{(2)}_2=u^{(2)}_{1,11}=u^{(2)}_{2,11}=0$ in the equations for the second mode and solve the resulting simplified equations for $u^{(2)}_1$ and $u^{(2)}_2$. Substituting these into equations for the lowest mode, we find

$$2b\left(c_{11}u^{(0)}_{1,11}+\frac{1}{b}c_{12}u^{(1)}_{2,1}\right)+(\sigma^{+}_{21}-\sigma^{-}_{21})=2b\rho\ddot{u}^{(0)}_1$$

$$2bc_{66}\left(\frac{1}{b}u^{(1)}_{1,1}+u^{(0)}_{2,11}\right)+(\sigma^{+}_{22}-\sigma^{-}_{22})=2b\rho\ddot{u}^{(0)}_2$$

$$\frac{2b}{3}\hat{c}_{11}u^{(1)}_{1,1}-2c_{66}\left(\frac{1}{b}u^{(1)}_1+u^{(0)}_{2,1}\right)+\frac{c_{12}}{3c_{22}}b(\sigma^{+}_{22}-\sigma^{-}_{22})_{,1}$$
$$+(\sigma^{+}_{21}+\sigma^{-}_{21})=\frac{2}{3}b\rho\ddot{u}^{(1)}_1$$

$$-2\left(c_{12}u^{(0)}_{1,1}+\frac{1}{b}c_{22}u^{(1)}_2\right)+(\sigma^{+}_{22}+\sigma^{-}_{22})$$
$$+\frac{b}{3}(\sigma^{+}_{21}-\sigma^{-}_{21})_{,1}=\frac{2}{3}b\rho\ddot{u}^{(1)}_2 \tag{7}$$

where + and − represent the stress components on the $\xi=1$ and $\xi=-1$ surfaces, respectively. This process decouples the stretching and bending motions of each layer. Note, however, that coupling of stretching and bending of the $N$-layered plate is included through the imposition of interface continuity conditions between layers.

### Plate Analysis

Since we now have a linear expansion for the displacement field, the displacements on both sides of a layer can be written as $u^{\pm}_i=\{u^{(0)}_i P_0(\xi)+u^{(1)}_i P_1(\xi)\}_{\xi=\pm 1}$. Remembering that the preceeding equations of motion are obtained for any arbitrary layer in the plate, say the $n$th layer, we can set $(\,)^{+}=(\,)_n$ and $(\,)^{-}=(\,)_{n-1}$. Then Eq. (7) can be im-

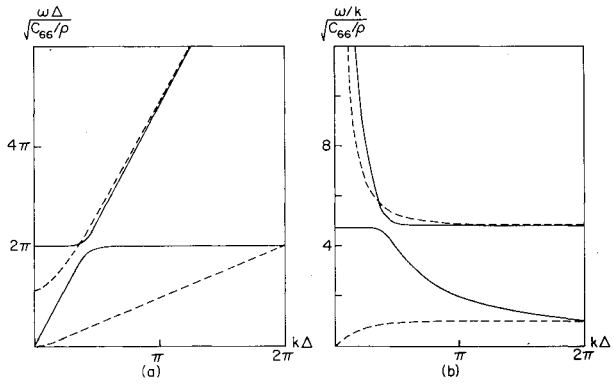


Fig. 2 Dispersion relationship and phase velocity of anisotropic plate: one-layer model (55% graphite fiber-epoxy matrix; layup angle 45 deg).

mediately written as

$$\rho(\ddot{u}_n+\ddot{u}_{n-1}) = c_{11}(u_n+u_{n-1})_{,11} + \frac{c_{12}}{b}(v_n-v_{n-1})_{,1} + \frac{1}{b}(\tau_n-\tau_{n-1})$$

$$\rho(\ddot{v}_n-\ddot{v}_{n-1}) = -\frac{3}{b}c_{12}(u_n+u_{n-1})_{,1} - \frac{3c_{22}}{b^2}(v_n-v_{n-1}) + \frac{3}{b}(\sigma_n+\sigma_{n-1}) + (\tau_n-\tau_{n-1})_{,1}$$

$$\rho(\ddot{u}_n-\ddot{u}_{n-1}) = \hat{c}_{11}(u_n-u_{n-1})_{,11} - \frac{3c_{66}}{b^2}(u_n-u_{n-1}) - \frac{3}{b}(v_n+v_{n-1})_{,1} + \frac{c_{12}}{c_{22}}(\sigma_n-\sigma_{n-1})_{,1} + \frac{3}{b}(\tau_n-\tau_{n-1})$$

$$\rho(\ddot{v}_n+\ddot{v}_{n-1}) = c_{66}\left\{\frac{1}{b}(u_n-u_{n-1})_{,1} + (v_n+v_{n-1})_{,11}\right\} + \frac{1}{b}(\sigma_n-\sigma_{n-1}) \qquad n=1,2,\ldots,N \tag{8}$$

where $\sigma$ and $\tau$ are used to represent $\sigma_{22}$ and $\sigma_{12}$ and $u$ and $v$ denote $u_1$ and $u_2$, respectively. These equations are the final approximate equations of motion of a layer written in the form of difference-differential equations.

In Eq. (8) we notice two important points. The first is that variation through the plate thickness is now discretized. Effectively we are using a finite-element substructuring in the thickness direction, while keeping the in-plane coordinate and time as continuous variables to which an integral transform technique can be applied. The second point concerns the continuity conditions of stress and displacement. These conditions require that $u$, $v$, $\sigma_{22}$, and $\sigma_{12}$ be continuous across the layer boundary. These conditions are identically satisfied by Eq. (8). The normal stress $\sigma_{11}$ tangential to the layer boundary is not necessarily continuous. Equation (8) allows such a discontinuity in $\sigma_{11}$.

## III. Dispersion Relations and Correction Factors

### Dispersion Relations

Calculation of dispersion relations is not necessary to find the transient solutions; however, they yield useful information about the correction factors. Correction factors are used in approximate theories of plates to match the thickness mode frequencies with those calculated from the exact theory.[7] For harmonic waves propagating in the $x_1$ direction, we assume $\exp[i(\omega t-kx_1)]$ type solutions, insert them onto Eq. (8), and apply the traction-free boundary conditions at $x_2=\pm b$ (or $x_2=\pm\Delta/2$). To this end, we obtain the following dispersion relations for a plate modeled with a single layer:

$$c_{11}\kappa^2 - \tfrac{1}{3}(\bar{\omega}^2-3c_{22})(\bar{\omega}^2-c_{11}\kappa^2)=0$$

$$c_{66}\kappa^2 - \tfrac{1}{3}(\bar{\omega}^2-c_{11}\kappa^2-3c_{66})(\bar{\omega}^2-c_{66}\kappa^2)=0 \tag{9}$$

where $\kappa=kb$ and $\bar{\omega}^2=\rho b^2\omega^2$. It is noted here that the first relationship corresponds to thickness extension (or the symmetric mode) and the second to the flexural deformation (or the antisymmetric mode). The exact theory of the plate gives an infinite number of dispersion relations. The present one-layer model, which is equivalent to the first-order approximation of Mindlin,[7,8] predicts the first four relations.

Dispersion relations and the corresponding phase velocities of a composite plate made of 55% graphite fiber-epoxy matrix with layup angles $\pm 45$ deg (see the Appendix for the elastic modulus) are shown in Fig. 2, up to a range where the wavelength becomes equal to the plate thickness. Solid lines represent the symmetric mode and dotted lines the antisymmetric mode. As we see in this figure, the phase velocities of the optical branch of both modes approach $(c_{11}/\rho)^{1/2}$ (i.e., the dilatation wave for an isotropic solid or the quasidilatation wave for an anisotropic solid), while those of the acoustic branch become $(c_{66}/\rho)^{1/2}$ (i.e., the shear wave for an isotropic solid or the quasishear wave for an anisotropic solid) when $k\to\infty$. The two cutoff frequencies of the optical branch are given by $(3c_{22}/\rho)^{1/2}2/\Delta$ for the symmetric mode and $(3c_{66}/\rho)^{1/2}2/\Delta$ for the antisymmetric mode. Similar behavior is also observed in a two-layer model.[16]

### Correction Factors

As is well understood, the shear wave (or the quasishear wave) limit at $k\to\infty$ and the cutoff frequencies are incorrect due to the linear approximation of the displacement in the plate. Such a discrepancy can be eliminated by introduction of correction factors as suggested by Mindlin and Medick[7,8]—the lowest cutoff frequencies of both modes of the approximate theory are set equal to the corresponding cutoff frequencies of the exact theory.‡

The lowest cutoff frequencies of the exact theory of the plate are $(\pi/\Delta)(c_{22}/\rho)^{1/2}$ for the quasidilatation wave and $(\pi/\Delta)(c_{66}/\rho)^{1/2}$ for the quasishear wave. The present approximate theory predicts $(2/\Delta)(c_{22}/\rho)^{1/2}$ and $(2/\Delta)(c_{66}/\rho)^{1/2}$. Hence we notice that when $c_{22}$ and $c_{66}$ of the approximate theory are replaced by $(\pi^2/12)c_{22}$ and $(\pi^2/12)c_{66}$, this theory now predicts not only the correct cutoff frequencies of both modes but also an identical large wave number limit, i.e., $(\pi/\sqrt{12})(c_{66}/\rho)^{1/2}=0.905\ (c_{66}/\rho)^{1/2}$, instead of $(c_{66}/\rho)^{1/2}$ for one of the antisymmetric modes when $k\to\infty$. Namely, we find a Rayleigh wave behavior replacing the incorrect shear wave behavior.

Another important result from the application of the correction factor $\pi^2/12$ occurs in the transient wave propagation. This will be discussed later.

## IV. Impact on Plate

### Difference Equation

When we apply a Laplace transform in a nondimensional time and a Fourier transform in a nondimensional space coordinate, Eq. (8) becomes

$$\left(fs^2+\frac{C_{11}}{2N}k^2\right)(\hat{\bar{U}}_n+\hat{\bar{U}}_{n-1}) + C_{12}ik \times(\hat{\bar{V}}_n-\hat{\bar{V}}_{n-1}) - (\hat{\bar{T}}_n-\hat{\bar{T}}_{n-1})=0$$

$$C_{12}ik(\hat{\bar{U}}_n+\hat{\bar{U}}_{n-1}) - \left(\frac{fs^2}{3}+2NC_{22}\right)(\hat{\bar{V}}_n-\hat{\bar{V}}_{n-1}) + (\hat{\bar{\Sigma}}_n+\hat{\bar{\Sigma}}_{n-1}) - \frac{ik}{6N}(\hat{\bar{T}}_n-\hat{\bar{T}}_{n-1})=0$$

$$C_{66}ik(\hat{\bar{U}}_n-\hat{\bar{U}}_{n-1}) + \left(fs^2+\frac{C_{66}}{2N}k^2\right) \times(\hat{\bar{V}}_n+\hat{\bar{V}}_{n-1}) - (\hat{\bar{\Sigma}}_n-\hat{\bar{\Sigma}}_{n-1})=0$$

$$\left(\frac{fs^2}{3}+\frac{\hat{C}_{11}k^2}{6N}+2NC_{66}\right)(\hat{\bar{U}}_n-\hat{\bar{U}}_{n-1}) + C_{66}ik(\hat{\bar{V}}_n+\hat{\bar{V}}_{n-1}) - \frac{C_{12}ik}{6NC_{22}}(\hat{\bar{\Sigma}}_n-\hat{\bar{\Sigma}}_{n-1}) + (\hat{\bar{T}}_n+\hat{\bar{T}}_{n-1})=0 \tag{10}$$

‡When the approxmate theory predicts the correct cutoff frequencies, the correction factor still can be used to improve the accuracy (see Ref. 9).

where ( $\hat{}$ ) represents a Laplace and Fourier transform of ( ). (Note; $C_{66} = 1$).

Since the simultaneous difference equations just given are linear and all the coefficients are constants, the solution has to be[17]:

$$\{\hat{U}_n, \hat{V}_n, \hat{T}_n, \hat{\Sigma}_n\} = \{A, B, C, D\} e^{2i\theta n} \tag{11}$$

where the phase shift $\theta$ is a complex number. Propagation through the thickness of the plate is characterized by $\theta$; that is, $2\theta$ is the wave number in the thickness direction. By substituting Eq. (11) into the difference equation, Eq. (10), we obtain a set of four simultaneous homogeneous equations through which we obtain the following equation for phase shift $\theta$:

$$\begin{aligned}
&\cos^4\theta\left(fs^2 + \frac{C_{11}k^2}{2N}\right)\left(fs^2 + \frac{C_{66}}{2N}k^2\right) + \sin^4\theta\left(\frac{fs^2}{3} + 2NC_{66} - \frac{C_{12}k^2}{6N}\right)\cdot\left(\frac{fs^2}{3} + \frac{\hat{C}_{11}}{6N}k^2 + 2NC_{66} - \frac{C_{66}}{6N}\,\frac{C_{12}}{C_{22}}k^2\right) \\
&+ \cos^2\theta\cdot\sin^2\theta\left[\left(fs^2 + \frac{C_{11}}{2N}k^2\right)\left\{\frac{k^2}{6N}C_{66} + \frac{fs^2}{3} + 2NC_{22} - \left(\frac{k}{6N}\right)^2\frac{C_{12}}{C_{22}}\left(fs^2 + \frac{C_{66}}{2N}k^2\right)\right\} - (C_{12}+C_{66})^2k^2\right. \\
&\left. + \left(fs^2 + \frac{C_{66}}{2N}k^2\right)\left(\frac{fs^2}{3} + \frac{\hat{C}_{11}k^2}{6N} + 2NC_{66} + \frac{C_{12}^2k^2}{6NC_{22}}\right)\right] = 0
\end{aligned} \tag{12}$$

This equation implies that for a given wave number $k$ and a frequency $s$ ($s$ represents the frequency in the case of harmonic waves), there exists an infinite set of values of wave numbers for propagation through the thickness direction. However, only two of them, $\beta$ and $\alpha$, are enough for $\cos^2\theta$ due to the periodic nature of Eq. (12) representing the quasishear wave and the quasidilatation wave. Furthermore, we notice that $-\beta$ and $-\alpha$ also satisfy the same phase shift equations but yield linearly independent solutions of the type given in Eq. (11). This clearly implies that for each wave we should have an incoming and outgoing wave front. Therefore, the general solutions of the difference equation, Eq. (10), should consist of four parts: $e^{2i\beta n}$, $e^{-2i\beta n}$, $e^{2i\alpha n}$, and $e^{-2i\alpha n}$.

Next, by substituting these solutions into the original difference equations we find the amplitude ratios among $A$, $B$, $C$, and $D$. Hence,

$$\begin{bmatrix}\hat{U}_n\\ \hat{V}_n\\ \hat{T}_n\\ \hat{\Sigma}_n\end{bmatrix} = \begin{bmatrix}X_1(\beta)E_1\\ X_2(\beta)E_2\\ X_3(\beta)E_2\\ E_1\end{bmatrix}\cdot\cos 2\beta n + i\begin{bmatrix}X_1(\beta)E_2\\ X_2(\beta)E_1\\ X_3(\beta)E_1\\ E_2\end{bmatrix}\cdot\sin 2\beta n + \begin{bmatrix}Y_1(\alpha)E_4\\ Y_2(\alpha)E_3\\ E_3\\ Y_3(\alpha)E_4\end{bmatrix}\cdot\cos 2\alpha n + i\begin{bmatrix}Y_1(\alpha)E_3\\ Y_2(\alpha)E_4\\ E_4\\ Y_3(\alpha)E_3\end{bmatrix}\cdot\sin 2\alpha n \tag{13}$$

where the amplitude ratio $X_i(\beta)$ and $Y_i(\alpha)$ are given by

$$\begin{aligned}
X_i(\beta) &= -\frac{\Delta_i(\beta)}{\Delta(\beta)} \\
\Delta(\beta) &= \left(fs^2 + \frac{C_{11}}{2N}k^2\right)\left(fs^2 + \frac{C_{66}}{2N}k^2\right)\cos^3\beta + \left\{\left(fs^2 + \frac{C_{66}}{2N}k^2\right)\left(\frac{fs^2}{3} + \frac{\hat{C}_{11}}{6N}k^2 + 2NC_{66}\right) - C_{66}C_{12}k^2 - C_{66}^2k^2\right\}\sin^2\beta\cdot\cos\beta \\
\Delta_1(\beta) &= ik\sin^2\beta\cdot\cos\beta\left\{\frac{C_{12}}{6NC_{22}}\left(fs^2 + \frac{C_{66}}{2N}k^2\right) - (C_{12}+C_{66})\right\} \\
\Delta_2(\beta) &= i\cdot\sin^3\beta\left\{\frac{C_{66}C_{12}}{6NC_{22}}k^2 - \left(\frac{fs^2}{3} + \frac{\hat{C}_{11}}{6N}k^2 + 2NC_{66}\right)\right\} - i\cos^2\beta\sin\beta\left(fs^2 + \frac{C_{11}}{2N}k^2\right) \\
\Delta_3(\beta) &= \sin^3\beta\cdot k\left\{\left(\frac{fs^2}{3} + \frac{\hat{C}_{11}}{6N}k^2 + 2NC_{66}\right)C_{12} - \frac{C_{12}^2k^2}{6NC_{22}}C_{66}\right\} \\
&\quad + \sin\beta\cdot\cos^2\beta\cdot k\left\{\frac{C_{12}}{6NC_{22}}\left(fs^2 + \frac{C_{11}k^2}{2N}\right)\cdot\left(fs^2 + \frac{C_{66}}{2N}k^2\right) - \left(fs^2 + \frac{C_{11}}{2N}k^2\right)C_{66}\right\}
\end{aligned} \tag{14}$$

and

$$\begin{aligned}
Y_i(\beta) &= -\bar{\Delta}_i(\alpha)/\bar{\Delta}(\alpha) \\
\bar{\Delta}(\alpha) &= i\cdot\cos^2\alpha\cdot\sin\alpha\left\{C_{66}k^2(C_{12}+C_{66}) - \left(fs^2 + \frac{C_{66}}{2N}k^2\right)\cdot\left(\frac{fs^2}{3} + \frac{\hat{C}_{11}k^2}{6N} + 2NC_{66} + \frac{C_{12}^2k^2}{6NC_{22}}\right)\right\} \\
&\quad + i\cdot\sin^3\alpha\left(\frac{fs^2}{3} + 2NC_{22}\right)\left(\frac{C_{66}C_{12}k^2}{6NC_{22}} - \frac{fs^2}{3} - \frac{C_{11}k^2}{6N} - 2NC_{66}\right) \\
\bar{\Delta}_1(\alpha) &= \cos^3\alpha\left(fs^2 + \frac{C_{66}}{2N}k^2\right) + \sin^2\alpha\cdot\cos\alpha\left\{-\left(\frac{k}{6N}\right)^2\frac{C_{12}}{C_{22}}\left(fs^2 + \frac{C_{66}}{2N}k^2\right) + \frac{k^2}{6N}C_{66} + \left(\frac{fs^2}{3} + 2NC_{22}\right)\right\}
\end{aligned}$$

$$\tilde{\Delta}_2(\alpha) = k\cdot\cos^2\alpha\cdot\sin\alpha(C_{12}+C_{66}) + k\cdot\sin^3\alpha\left\{\frac{1}{6N}\left(\frac{fs^2}{3}+\frac{\hat{C}_{11}k^2}{6N}+2NC_{66}\right)-\left(\frac{k}{6N}\right)^2\frac{C_{12}C_{66}}{C_{22}}\right\}$$

$$\tilde{\Delta}_3(\alpha) = ik\cdot\sin^2\alpha\cdot\cos\alpha\left\{\frac{C_{66}^2}{6N}k^2-\frac{1}{6N}\left(\frac{fs^2}{3}+\frac{\hat{C}_{11}k^2}{6N}+2NC_{66}\right)\left(fs^2+\frac{C_{66}}{2N}k^2\right)\right.$$

$$\left.+C_{66}k\left(\frac{fs^2}{3}+2NC_{22}\right)\right\}-ik\cdot\cos^3\alpha\cdot C_{12}\left(fs^2+\frac{C_{66}}{2N}k^2\right) \tag{15}$$

Equations (13-15) with the phase shifts $\alpha$ and $\beta$ constitute the general solutions of the governing difference equations, Eq. (10).

In view of Eqs. (14) and (15), we notice that when $k\to 0$ we have $X_1(\beta)=X_3(\beta)=Y_1(\alpha)=Y_3(\alpha)=0$. Namely, for a plane wave propagating normal to the layers the quasidilatation wave with a phase shift $\beta$ and the quasishear wave with a phase shift $\alpha$ are completely uncoupled and become the dilatation wave and the shear wave as expected.

**Impact Boundary Condition**

For the present problem we have chosen a line impact of a normal stress along the $x_3$ axis at $x_2=-b$ given as

$$\sigma_0 = -\frac{P_0}{4}\left(1-\cos\frac{2\pi t}{t_0}\right)\cdot\left(1+\cos\frac{\pi x}{a}\right) \qquad |x_1|<a \text{ and } 0<t<t_0$$

$$=0 \qquad |x_1|>a \text{ or } t>t_0$$

$$\tau_0 = \sigma_N = \tau_N = 0$$

Hence, the boundary conditions for the present impact problem leads to the following equation§:

$$\begin{bmatrix} 0 & X_3(\beta) & 1 & 0 \\ 1 & 0 & 0 & Y_3(\alpha) \\ iX_3(\beta)\sin2\beta N & X_3(\beta)\cos2\beta N & \cos2\alpha N & i\sin2\alpha N \\ \cos2\beta N & i\sin2\beta N & iY_3(\alpha)\sin2\alpha N & Y_3(\alpha)\cos2\alpha N \end{bmatrix}\begin{bmatrix} E_1 \\ E_2 \\ E_3 \\ E_4 \end{bmatrix} = \begin{bmatrix} 0 \\ \hat{\bar{\sigma}}_0 \\ 0 \\ 0 \end{bmatrix} \tag{17}$$

Upon solving the above equations for $E_i$'s and substituting them into Eq. (13), we can find the complete solution which satisfies the given impact boundary conditions. For given values of $k$ and $s$, we first calculate the phase shift $\alpha$ and $\beta$ from Eq. (12). Using these $\alpha$ and $\beta$ in Eqs. (13-15), we obtain the general solution. Next, the particular solution satisfying the impact condition is found by computing the $E_i$'s from Eq. (17). After the transformed quantities $\hat{\bar{U}}_n$, $\hat{\bar{V}}_n$, $\hat{\bar{T}}_n$, and $\hat{\bar{\Sigma}}_n$ have been calculated for a given impact function, they can be inverted easily by means of a Fast Fourier Transform routine[2,16] to give the transient displacement and stress propagation after impact.

Here we notice an interesting point. If more accurate distribution of the stress and displacement field are necessary through the plate thickness, they can be obtained by increasing the layer number $N$. The major advantage of the present theory is that neither additional analysis in the formulation nor more computation time to invert a larger matrix is necessary. Additional computation time is required only to calculate Eq. (13) at more points and to invert the integral transform, which requires little extra time.

## V. Numerical Results

**Case 1. Longitudinal Propagation**

Propagation of impact-generated waves along the longitudinal ($x_1$) direction is first examined for an isotropic plate ($\lambda=\mu=1.2\times10^7$ psi) employing a two-layered model. For these calculations we used an impact time $t_0=10$ $\mu$s, plate thickness $\Delta=1$ cm, and impact width $a=4$ cm. Some of the results at a few different time steps are shown in Fig. 3, $a\sim f$.

In these figures, we can see two distinct states of propagation and corresponding wave fronts—one for longitudinal displacement $u_n$ and longitudinal normal stress $\sigma_{11_n}$ and another for transverse displacement $v_n$ and shear stress $\tau_n$. In other words, the initial signals of the displacement $u_n$ and, accordingly, the longitudinal normal stress $\sigma_{11}$ propagate first along the plate, and the shear stress and the displacement $v_n$ follow next. When the group velocities are calculated from the numerical results, they are about 5 and 3 mm/$\mu$s, respectively, while the phase velocities of the unbounded medium of this material are $C_d=\sqrt{(\lambda+2\mu)/\rho}=5.61$ mm/$\mu$s and $C_s\sqrt{\mu/\rho}=3.25$ mm/$\mu$s, thus showing the dispersive nature of the plate due to the boundary.

A relatively insignificant part of the stress propagates via dilatational and shear waves. The maximum stress is transmitted by a bending wave which propagates in the plate at a much slower speed.

**Case 2. Propagation through the Thickness**

To examine the propagation through the thickness it is necessary to have a sufficient number of layers in a plate. It is also important to make the time step smaller than the required time for waves to travel through a layer thickness. To do this we increase the thickness of the plate and number of layers and reduce the impact time.

In Fig. 4 transverse propagation of the normal stress is shown for a time sequence in an anisotropic plate with effective moduli of 55% graphite fiber-epoxy matrix composite at a layup angle of 15 deg. The eight-layer model has a thickness of 1 cm and the impact time is 2 $\mu$s. In this figure, we see that the transverse normal stress is initially compressive at $x_2=-\Delta/2$ due to the impact and a compression wave propagates through the thickness. Later it becomes a tension wave after reflection from the free surface and the tension wave propagates back to the impact surface. Here we also notice a clear delay in time for waves to travel from one layer to the next. Another important point is that the shape of the impact stress is relatively well preserved during the initial

§If we set the determinant of the coefficient matrix equal to zero, this condition leads to dispersion relations of an $N$-layer plate.

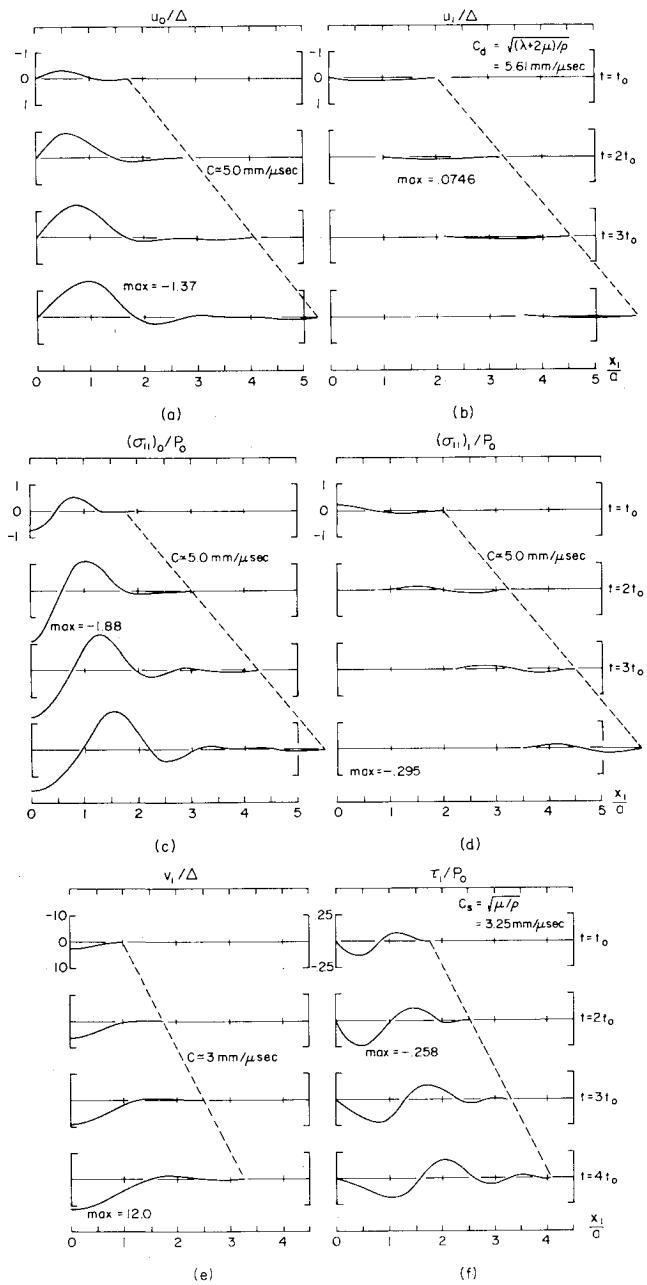


**Fig. 3 Longitudinal propagation of impact stress in isotropic plate: two-layer model ($\lambda = \mu = 1.2^* 10^7$ psi; $\Delta = 1$ cm, $t_0 = 10$ μs, $a = 4$ cm).**

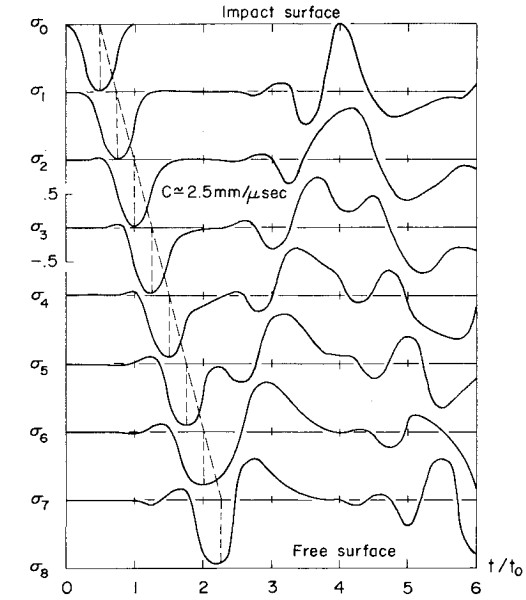


**Fig. 4 Transverse propagation of normal stress in an anisotropic plate: eight-layer model (55% graphite fiber-epoxy matrix; layup angle 15 deg; $\Delta = 1$ cm, $t_0 = 2$ μs, $a = 2$ cm).**

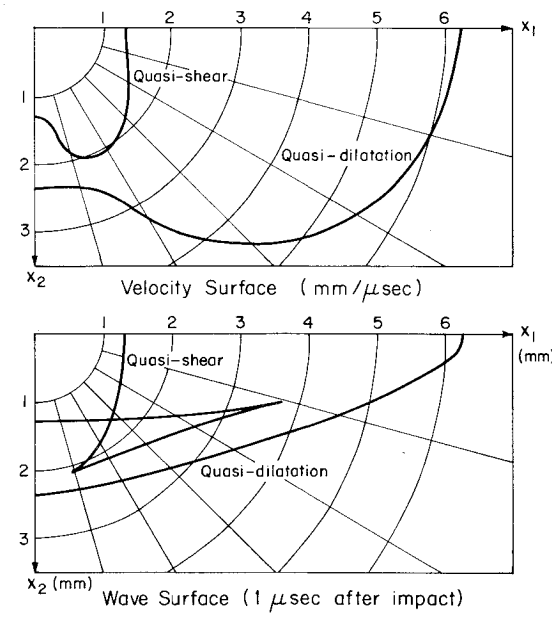


**Fig. 5 Velocity surfaces and wave surface of anisotropic plate (55% graphite fiber-epoxy matrix; layup angle 45 deg).**

stage of propagation by changes immediately afterwards. The distortion of the shape becomes more serious with further propagation due to reflection, thus showing the highly dispersive nature of the harmonic waves.

### Case 3. Wave Surfaces

When the medium is anisotropic, the phase velocity varies from one direction to another. As a result of such a variation, the wave fronts are no longer circles but have rather complicated shapes.[1,15]

The velocity and wave surfaces of an anisotropic plate, with effective moduli of a graphite fiber-epoxy matrix composite are shown in Fig. 5. For the line impact problem we have a distributed source of waves over the impact region $-a \le x_1 \le a$. The wave fronts of the distributed source are the envelopes of each wave front from every point in the impact area. The enveloped wave fronts (calculated theoretically) and the stress state in the composite plate at 10 μs after the impact are shown in Fig. 6. Here we notice that the propagation of a normal stress is well bounded by the quasidilatational wave front, but the longitudinal propagation of the shear stress is not bounded within the quasishear wave surface. This implies that although the major part of the shear stress propagates with the quasishear wave, a considerable part of it propagates with the quasidilatational wave.

### Effect of Correction Factors on Transient Waves

The purpose of the correction factors for $c_{22}$ and $c_{66}$ in the study of dispersion, i.e., to match the cutoff frequencies[7,8] or the slopes of the dispersion relations[9] with those of the exact theory, has been demonstrated by many authors. Now their effects on propagation through the thickness direction and transient waves are self-evident. Namely, propagation speeds through the thickness $(c_{22}/\rho)^{1/2}$ and $(c_{66}/\rho)^{1/2}$ are reduced by a factor of $\pi/\sqrt{12}$ as shown in Fig. 7. In this figure, propagation of the peak value of the interlaminar normal

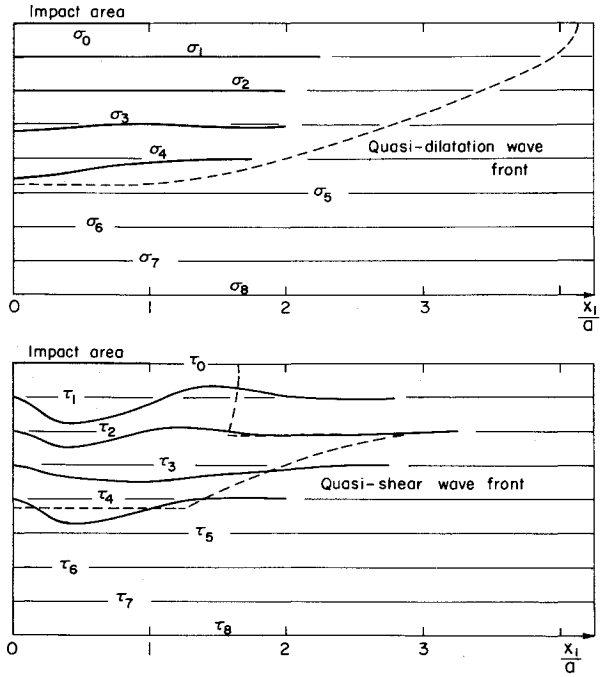


**Fig. 6 Comparison of theoretical wave front and numerical wave front of anisotropic plate (55% graphite fiber-epoxy matrix; layup angle 45 deg; 10 $\mu$s after impact for numerical results; eight-layer model, $\Delta = 4$ cm, $t_0 = 4$ $\mu$s, $a = 2$ cm).**

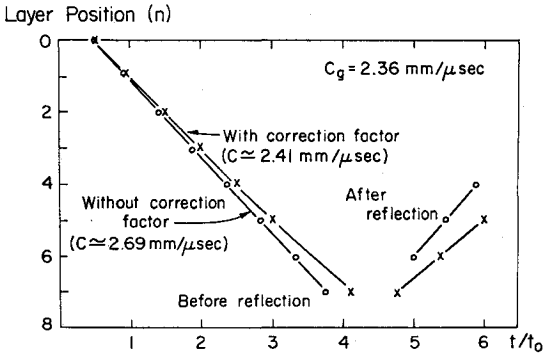


**Fig. 7 Effect of correction factors on transverse propagation of max $\sigma_n(x_1 = 0)$; eight-layer model (55% graphite fiber-epoxy matrix; layup angle 45 deg; $\Delta = 4$ cm, $t_0 = 4$ $\mu$s, $a = 2$ cm).**

stress from the impact surface through the plate thickness is shown. The layer position $n$ vs time at which $\sigma_n(x_1 = 0)$ becomes maximum is plotted. Without the correction factors, the propagation speed is about 2.69 mm/$\mu$s, which exceeds $(c_{22}/\rho)^{1/2} = 2.36$ mm/$\mu$s, the exact propagation speed of a quasidilatational wave through the thickness. When the correction factors are introduced, this speed is reduced to 2.41 mm/$\mu$s. The same phenomenon is observed in Fig. 4: the propagation speed is reduced from 2.5 to 2.25 mm/$\mu$s when the correction factors are applied. Results without the correction factors predict wave propagation beyond the wave surface estimated by the exact theory as shown in Ref. 16. Such a discrepancy is removed by application of the correction factors.

For a two-layered plate, the present theory predicts two cutoff frequencies for each of the two deformation modes. The second cutoff frequency of the symmetric mode is twice the first cutoff frequency of the antisymmetric mode[16] as in the exact thory. Therefore, adjusting the lower cutoff frequency of the symmetric mode by a correction factor also matches the higher cutoff frequency of the antisymmetric mode and vice versa. Thus, two correction factors adjust all four cutoff frequencies of the approximate theory. However, this is not true for a plate made of more than two layers. For example, only the 2, 4, 6, . . . $N$th ($N$: even integer) cutoff frequencies of each mode are equal to those of the exact theory, while the 1, 3, . . . ($N$-1)th cutoff frequencies are still different. In other words, two correction factors are not enough to adjust all cutoff frequencies and their consequences, which is quite natural to an approximate theory. As a result of this phenomenon, we have a slight difference in the propagation speed through the thickness of the plate as shown in Fig. 7. The propagation speed from the numerical result, 2.41 mm/$\mu$s is still higher than $(c_{22}/\rho)^{1/2} = 2.36$ mm/$\mu$s, and this difference cannot be corrected in a simple manner. Fortunately, the error of the present theory is small ($\sim 2\%$ in the case of Fig. 7 which shows the worst case among all the numerical results obtained in the present work).

## VI. Conclusions and Summary

Propagation of stress waves in a homogeneous anisotropic plate has been examined by a combined use of the finite-element technique in the plate thickness direction and the Fast Fourier Transform in the plane of plate and in time.

The present theory has the following advantages over previously reported research: 1) calculation of dispersion relations is not necessary to find the transient solutions; 2) increasing the number of layers does not lead to increased algebraic complexity or significantly increased computer run times; 3) propagation of waves through the plate thickness can be examined in a simple way; 4) application of the FFT method permits arbitrary initial conditions and distributed loading in a more efficient way than do other numerical algorithms, such as those based on modal superposition,[12] and two- or three-dimensional discretization methods. However, some attention must be paid in the use of the FFT with regard to determination of proper time and space steps (frequency and wave number steps in the transformed space).[2,18]

### Discussion of Computation Time

It is interesting to compare the computation time for this model with some other methods, such as the finite-element or finite-difference methods. In the case of an eight-layer anisotropic plate model from which Figs. 4 and 6 are produced, we have

| | |
|---|---|
| 9 steps through the thickness: | 8-layer model |
| 32 steps in the $x_1$ direction: | 64 points are used in the FFT but only half of them are useful because of the symmetry of problem. |
| 32 steps in time with two displacement components at each point. | |

Therefore, the total numer of the primary unknowns is 18,432. After these primary variables have been calculated, 27,648 secondary variables (three stress components at each point) must be calculated. For the preceding model, all of these calculations require only 200 K of computer core. Magnetic tapes or any kind of additional data storage devices are not required. Only 66 CPU seconds are required for execution on the IBM 370-168 computer.

A comparison of the theoretical model with the use of the Fast Fourier Transform with classical plate results for one layer has been made in Ref. 3. Comparison of our multilayer model using the FFT with other numerical methods is difficult, since only a few transient multilayer plate analyses can be found in the literature. We found only one such example suitable for comparison—a modal analysis by Kubo and

Nelson[12] of a two-layered plate under a triangular ramp impact force in time distributed in a half-sine wave over one surface of the plate.

In the Kubo-Nelson example, 50 modal solutions were found for different wavelengths along the beam. This took 37 min of computer time, 8 of which were for input and output on an IBM 360/91 computer. These 50 modal solutions were then used to find the transient response requiring 15 min of computer time, 10 of which were for input and output (i.e., writing on tapes).

In our method, 32 wavelengths along the plate were used for a nine-layer plate and the transient response was calculated in 66 s of CPU time on the IBM 370-168. We feel this is a significant improvement over the modal method. Unfortunately we did not have similar results for a finite-element method to compare our results with.

## Appendix—Effective Elastic Constants of 55% Graphite Fiber-Epoxy Matrix

$(c_{11}, c_{12}, c_{22}, c_{66}) * 10^6$ psi

±15 layup

$$\begin{bmatrix} 24.56 & 0.4000 & 0 \\ & 1.170 & 0 \\ & & 0.3552 \end{bmatrix}$$

±45 layup

$$\begin{bmatrix} 8.197 & 0.4279 & 0 \\ & 1.170 & 0 \\ & & 0.3552 \end{bmatrix}$$

## Acknowledgments

The present research has been supported by NASA Lewis Research Center. We wish to express our appreciation for the support of C.C. Chamis of NASA.

## References

[1] Moon, F. C., "Wave Surfaces Due to Impact on Anisotropic Plates," *Journal of Composite Materials*, Vol. 6, Jan. 1972, pp. 62-79.

[2] Moon, F. C., "Stress Wave Calculations in Composite Plates Using the Fast Fourier Transform," *Computers and Structures*, Vol. 3, 1973, pp. 1195-1204.

[3] Moon, F. C., "One Dimensional Transient Waves in Anisotropic Plates," *Journal of Applied Mechanics*, Vol. 40, June 1973, pp. 485-490.

[4] Moon, F. C., "Wave Propagation and Impact in Composite Materials," edited by C. C. Chamis, *Composite Materials*, Vol. 7, Academic Press, New York, 1975, Chap. 6.

[5] White, J. E. and Angona, F. A., "Elastic Wave Velocities in Laminated Media," *Journal of the Acoustical Society of America*, Vol 27, March 1955, pp. 310-317.

[6] Sun, C. T., Achenbach, J. D., and Herrmann, G., "Continuum Theory for a Laminated Media," *Journal of Applied Mechanics*, Vol. 35, Sept. 1968, pp. 467-475.

[7] Mindlin, R. D., "High Frequency Vibrations of Crystal Plates," *Quarterly of Applied Mathematics*, Vol. 19, No. 1, April 1961, pp. 51-61.

[8] Mindlin, R. D. and Medick, M. A., "Extensional Vibrations of Elastic Plates," *Journal of Applied Mechanics*, Vol. 26, Dec. 1959, pp. 561-569.

[9] Lee, P. C. Y. and Nikodem, Z., "An Approximate Theory for High-Frequency Vibrations of Elastic Plates," *International Journal of Solids and Structures*, Vol. 8, 1972, pp. 581-612.

[10] Dong, S. B. and Nelson, R. B., "On Natural Vibrations and Waves in Laminated Orthotropic Plates," *Journal of Applied Mechanics*, Vol. 39, Sept. 1972, pp. 739-745.

[11] Tiersten, M. F., *Linear Piezoelectric Plate Vibrations*, Plenum Press, New York, 1969, Chap. 12.

[12] Kubo, J. T. and Nelson, R. B., "Analysis of Impact Stresses in Composite Plates," American Society for Testing and Materials, Special Technical Publication 568, Philadelphia, Pa., 1975, pp. 228-244.

[13] Brillouin, L., *Wave Propagation in Periodic Structures*, Dover, N. J., 1965, Chap. 2, Dover Publ. Inc., N.Y., 1953.

[14] Thomson, W. T., *Vibration Theory and Application*, Prentice Hall, Englewood Cliffs, N. J., 1965, p. 245.

[15] Hermon, R. F. S., *An Introduction to Applied Anisotropic Elasticity*, Oxford University Press, 1961.

[16] Kim, B. S. and Moon, F. C., "Transient Wave Propagation in Composite Plates Due to Impact," *Proceedings of AIAA/ASME 18th Structures, Structural Dynamics and Materials Conference*, Vol. B, San Diego, Calif., March 1977, pp. 43-50.

[17] Levy, H. and Lessman, F., *Finite Difference Equations*, MacMillan, New York, 1961, Chap. 4.

[18] Cooley, J. W., Lewis, P. A. W., and Welch, P. D., "The Fast Fourier Transform Algorithm: Programming Considerations in the Calculation of Sine, Cosine and Laplace Transform," *Journal of Sound and Vibration*, Vol. 12, 1970, pp. 315-337.

[19] Brigham, E. O., *The Fast Fourier Transform*, Prentice Hall, Englewood Cliffs, N. J., 1974.